Reversible suppression of an essential gene in adult mice using transgenic RNA interference

Katherine McJunkin[a,b], Anthony Mazurek[a], Prem K. Premsrirut[a], Johannes Zuber[a,1], Lukas E. Dow[a], Janelle Simon[a], Bruce Stillman[a,b,2], and Scott W. Lowe[a,b,c,2]

[a]Cold Spring Harbor Laboratory, [b]Watson School of Biological Sciences, and [c]The Howard Hughes Medical Institute, Cold Spring Harbor, NY, 11724

Contributed by Bruce Stillman, March 17, 2011 (sent for review December 29, 2010)

RNAi has revolutionized loss-of-function genetics by enabling sequence-specific suppression of virtually any gene. Furthermore, tetracycline response elements (TRE) can drive expression of short hairpin RNAs (shRNAs) for inducible and reversible target gene suppression. Here, we demonstrate the feasibility of transgenic inducible RNAi for suppression of essential genes. We set out to directly target cell proliferation by screening an RNAi library against DNA replication factors and identified multiple shRNAs against Replication Protein A, subunit 3 (RPA3). We generated transgenic mice with TRE-driven Rpa3 shRNAs whose expression enforced a reversible cell cycle arrest. In adult mice, the block in cell proliferation caused rapid atrophy of the intestinal epithelium which led to weight loss and lethality within 8–11 d of shRNA induction. Upon shRNA withdrawal, villus atrophy and weight loss were fully reversible. Thus, shRpa3 transgenic mice provide an interesting tool to study tissue maintenance and regeneration. Overall, we have established a robust system that serves the purpose of temperature-sensitive alleles in other model organisms, enabling inducible and reversible suppression of essential genes in a mammalian system.

RNAi transgenics | gene targeting | mouse genetics | conditional knockout | mouse models

Loss-of-function experiments reveal the biological function of a gene of interest through the phenotype that results from its deficiency. The most dramatic phenotype is lethality, defining a gene as essential. Although such a striking phenotype places essential genes among the most interesting, it also renders them the most difficult class of genes to study. First, null alleles must be maintained as a heterozygous stock. Second, in homozygotes, the role of the gene can be studied only in the developmental stages preceding lethality. Thus, any function the gene might play later in development remains unknown. Additionally, the absence of a gene throughout development may induce compensatory shifts in related pathways, confounding the interpretation of results (1).

In simple model organisms, temperature-sensitive mutants isolated in forward genetic screens are crucial to studying essential genes. These lines can be maintained at permissive temperature, and simply shifting to restrictive temperature reveals the mutant phenotype. Thus, essential genes can be acutely and transiently inactivated at any stage in development.

Although such tools are not available in mouse models, conditional deletion alleles in which the gene of interest is flanked by loxP recombination sites enable acute gene inactivation upon expression of Cre recombinase. Expression of Cre from tissue-specific promoters yields gene deletion in a restricted compartment, whereas the use of tamoxifen-inducible Cre alleles allows precise timing of recombination. However, these approaches require costly and time-consuming generation of customized targeting cassettes and production of ES cells by homologous recombination. Also, Cre-mediated gene excision is incomplete, and the efficiency of excision varies with respect to the size of the targeted cassette (2). Furthermore, continuous expression of Cre can have genotoxic and/or mutagenic side effects, potentially confounding the interpretation of results, especially when studying DNA damage or metabolism (3–5). Most importantly, conditional gene deletion is not reversible, so these models cannot be used to determine the effect of transient gene inactivation, during windows of development or in the adult.

In recent years, RNAi has enabled fast and versatile loss-of-function studies in mammalian cells through transient transfection of synthetic small interfering RNAs or transduction of viral vectors that drive stable or inducible expression of shRNAs. In a transgenic setting, shRNA expression alleles recapitulate knockout mouse phenotypes when constitutively or inducibly expressed, thus providing an alternative to Cre-mediated gene deletion (6–14). Importantly, shRNAs under the control of the reversible tetracycline-responsive element (TRE) allow both inducible gene knockdown and rapid reactivation (15, 16). Moreover, shRNA transgenesis is faster than generation of conventional and conditional knockouts because it obviates the need for site-specific homologous recombination, and, because RNAi suppresses gene function in trans, only a single transgenic allele is necessary, thus reducing animal husbandry. Therefore, we envisaged inducible RNAi transgenics as an effective tool to dissect the role of essential genes in mice.

We recently developed a rapid, scalable platform for the generation of inducible shRNA transgenic mice and used it to study suppression and reactivation of tumor suppressor genes, whose inactivation promotes cancer development (17). Here, we address the challenge of targeting essential genes, a unique setting where expression of the shRNA could be deleterious, enforcing selective pressure against induction of the transgene. To determine whether this system would be sufficiently robust to induce lethal phenotypes and thus accurately assess essential gene function, we chose to inhibit an essential process by RNAi: DNA synthesis. Our results show that transgenic RNAi targeting the DNA replication machinery causes widespread inhibition of cell proliferation in adult mice, and thus dramatic phenotypes arise in highly proliferative tissues. More generally, our results establish a robust and versatile platform to study virtually any essential gene in mice.

Results

shRNAs Targeting RPA Strongly Inhibit Cell Proliferation. An shRNA screen was conducted in HCT116 colorectal carcinoma cells to identify genes involved in DNA synthesis that were sensitive to RNAi inhibition. A library of 254 shRNAs targeting genes with either established or suspected roles in DNA replication was cloned into a retroviral construct in the context of a human miR-30 transcript. For each shRNA, cells were transduced, selected with puromycin, and counted 5 d following transduction. Many

Author contributions: K.M., A.M., B.S., and S.W.L. designed research; K.M., A.M., and J.S. performed research; P.K.P., J.Z., and L.E.D. contributed new reagents/analytic tools; K.M. and A.M. analyzed data; and K.M., B.S., and S.W.L. wrote the paper.

Freely available online through the PNAS open access option.

P.K.P and S.W.L. are founders on the scientific advisory board of Mirimus, Inc., a company that has licensed technology related to this work.

[1]Present address: Research Institute of Molecular Pathology (IMP), A-1030 Vienna, Austria.

[2]To whom correspondence may be addressed E-mail: stillman@cshl.edu or lowe@cshl.edu.

This article contains supporting information online at www.pnas.org/lookup/suppl/doi:10.1073/pnas.1104097108/-/DCSupplemental.

shRNAs were identified that reduced cell number more than twofold compared with controls, including multiple shRNAs targeting PES1 and the RPA complex (Fig. 1 *A*–*C*). PES1 encodes a protein implicated in cell cycle progression and ribosome biogenesis (18, 19). RPA is the heterotrimeric single-stranded DNA binding complex that stabilizes replication forks by coating melted DNA; the RPA complex also binds ssDNA at sites of DNA damage and recruits cell cycle checkpoint kinases (reviewed in refs. 20 and 21). Two anti-proliferative shRNAs targeting the smallest RPA subunit, RPA3, induce degradation of all three members of the RPA complex, whereas RPA1 shRNA knocks down only its target (Fig. S1*A*). We chose to use RPA3 shRNAs in further studies because of its well characterized roles in DNA replication and repair and because its sole suppression destabilized the entire RPA complex. To study Rpa3 knockdown in transgenic mice, shRNAs were cloned that potently targeted mouse Rpa3 (Fig. S1*B*).

TREtight Prevents Sterility in shRpa3 Founder Mice. To facilitate the fast and reproducible generation of shRNA transgenic mice, we used a recently developed targeting cassette that enables efficient integration of an inducible shRNA transgene at a defined genomic locus (17, 22). This targeting vector consists of a miR-30-based shRNA embedded in the 3′ UTR of a GFP transcript downstream of the inducible TRE-CMV promoter (TRE; Fig. S1*C*). In this configuration, fluorescence reports the level of induction of the shRNA transcript.

Following electroporation of the targeting vector and a plasmid expressing Flpe recombinase into KH2 ES cells (22), recombinase-mediated cassette exchange promotes integration of the TRE-GFP-miR/shRNA (TGM) cassette into a defined locus downstream of the collagen A1 gene (ColA1; ref. 17). In addition to the ColA1 homing cassette, KH2 cells are also transgenic at the Rosa26 locus where a modified reverse tetracycline transactivator coding sequence (rtTA-M2) is knocked in downstream of the endogenous Rosa26 promoter (22, 23). rtTA drives strong reversible expression from the TRE promoter in the presence of the tetracycline analog doxycycline (dox) (24), allowing immediate testing of TRE function in targeted ES cells.

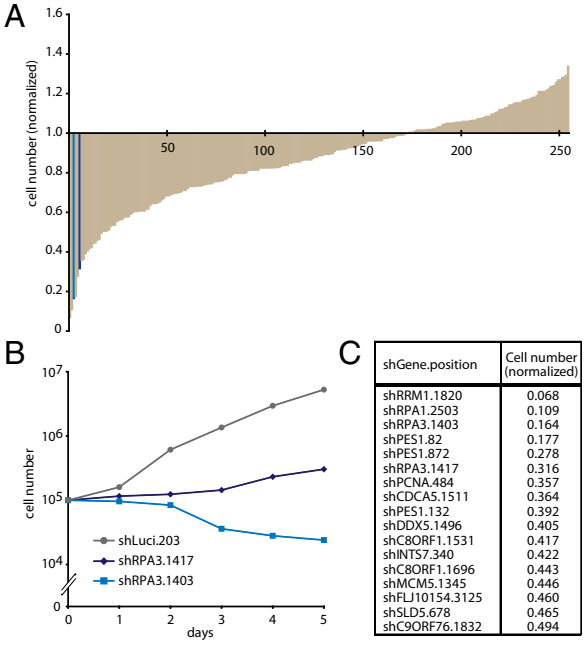

shGene.position	Cell number (normalized)
shRRM1.1820	0.068
shRPA1.2503	0.109
shRPA3.1403	0.164
shPES1.82	0.177
shPES1.872	0.278
shRPA3.1417	0.316
shPCNA.484	0.357
shCDCA5.1511	0.364
shPES1.132	0.392
shDDX5.1496	0.405
shC8ORF1.1531	0.417
shINTS7.340	0.422
shC8ORF1.1696	0.443
shMCM5.1345	0.446
shFLJ10154.3125	0.460
shSLD5.678	0.465
shC9ORF76.1832	0.494

Fig. 1. High-throughput RNAi screen identifies shRNAs that inhibit cell proliferation. (*A*) A library of 254 shRNAs targeting 83 known and putative replication factors was used to transduce HCT116 cells. Cells were selected in puromycin for 4 d, then counted to determine shRNA effects on cell proliferation. Cell number is normalized to cultures transduced with negative control shRNAs targeting EBNA1 or luciferase. Values corresponding to two RPA3 shRNAs are highlighted in blue. (*B*) Growth curve of cells transduced with two shRNAs targeting RPA3 or luciferase. (*C*) Hairpins that reduce HCT116 cell number greater than twofold.

Using this system, one weak (shRpa3.429) and one potent (shRpa3.455) shRNA against mouse Rpa3 were targeted to the ColA1 locus. As expected, dox treatment of each targeted clone induced strong GFP expression and knockdown of Rpa3, effects that were reversed when dox was withdrawn (Fig. S1*B*). Next, fully transgenic mice were generated by injecting these ES cells into tetraploid blastocysts. The resulting animals developed normally, but only transgenics harboring the weak TG-shRpa3.429 were fertile. Although the ES cells showed no GFP expression or Rpa3 knockdown in the absence of dox (Fig. S1*B*), we hypothesized that the sterility in strong TG-shRpa3.455 founders was caused by low levels of the shRpa3 inhibiting meiotic recombination during germline development, because Rpa is required for recombination. Furthermore, ES cells harboring inducible shRNAs targeting many nonessential genes yielded viable founder lines (17).

To circumvent this issue, the shRNA targeting construct was modified to contain a TREtight promoter (Tt), which shows 40-fold lower expression in the absence of dox than the conventional TRE promoter (25). The GFP spacer was also changed to a fast-maturing fluorescent protein (turboRFP; herein cited as tRFP) for rapid fluorescent detection of induction, to yield the final Tt-tRFP-miR/shRNA (TtRM) cassette. Additionally, a second strong Rpa3 shRNA was identified through a high-throughput assay of shRNA potency described elsewhere (26), and thus KH2 ES cells were targeted with two different potent Rpa3 shRNAs (shRpa3.455 and shRpa3.561) or a potent shRNA against firefly luciferase (shLuci) in TtRM. Again, tRFP was strongly induced by dox and reported concomitant Rpa3 knockdown in shRpa3-targeted ES cells, and both tRFP level and knockdown were quickly reversed upon dox withdrawal (Fig. 2*A Left*). These cells were used for tetraploid blastocyst complementation and yielded fertile founder lines, suggesting that TREtight prevented deleterious leaky expression of shRpa3.

Transgenic Rosa26-rtTA;TtR-shRpa3 MEFs Reversibly Arrest in Dox. As a first step in characterizing the functional consequences of Rpa3 inhibition in transgenic cells, mouse embryonic fibroblasts (MEFs) were isolated from embryos transgenic for both Rosa26-rtTA-M2 (Rosa-rtTA) and TtRM (23, 25) and examined for Rpa3 expression and proliferation in the absence or presence of dox. A 4-d pulse of dox treatment resulted in rapid, reversible induction of tRFP in all cells, along with Rpa3 knockdown in shRpa3 MEFs, but not shLuci MEFs (Fig. 2*A Right*). Accordingly, Rosa-rtTA; shRpa3 MEFs arrested after 4 d in dox (Fig. 2*B*), whereas those grown in the absence of dox continued to multiply similar to shLuci controls. Dox treatment did not result in a significant increase in apoptotic cells (Fig. S2). This defect in proliferation was completely reversible, as arrested cells resumed proliferation within days of dox withdrawal, eventually proliferating as rapidly as untreated controls (Fig. 2*C*).

To further characterize the nature of the shRpa3-induced cell cycle arrest, MEFs were BrdU-pulsed and analyzed by flow cytometry after 0, 2, 4, or 6 d of dox treatment. Cell cycle analysis of Rosa-rtTA;shRpa3 MEFs showed an accumulation of BrdU-negative cells with greater than 2C DNA content upon dox treatment, indicative of arrest in S phase (Fig. 2 *D* and *E*). In these cells, dox treatment induced phosphorylation of Chk2, but did not lead to a strong induction of gamma-H2A.X, indicating that the cell cycle arrest caused by Rpa3 knockdown is not the result of a DNA damage-induced cell cycle checkpoint caused by stalled replication (Fig. 2*F*).

To determine whether shRNA-mediated Rpa3 suppression was sufficient to interfere with checkpoint signaling, Rosa-rtTA; shRpa3 MEFs were treated with hydroyurea (HU) or ionizing radiation (IR). In the absence of dox, both HU and IR strongly induced phosphorylation of Chk1, Chk2, and H2A.X (Fig. 2*F*). In

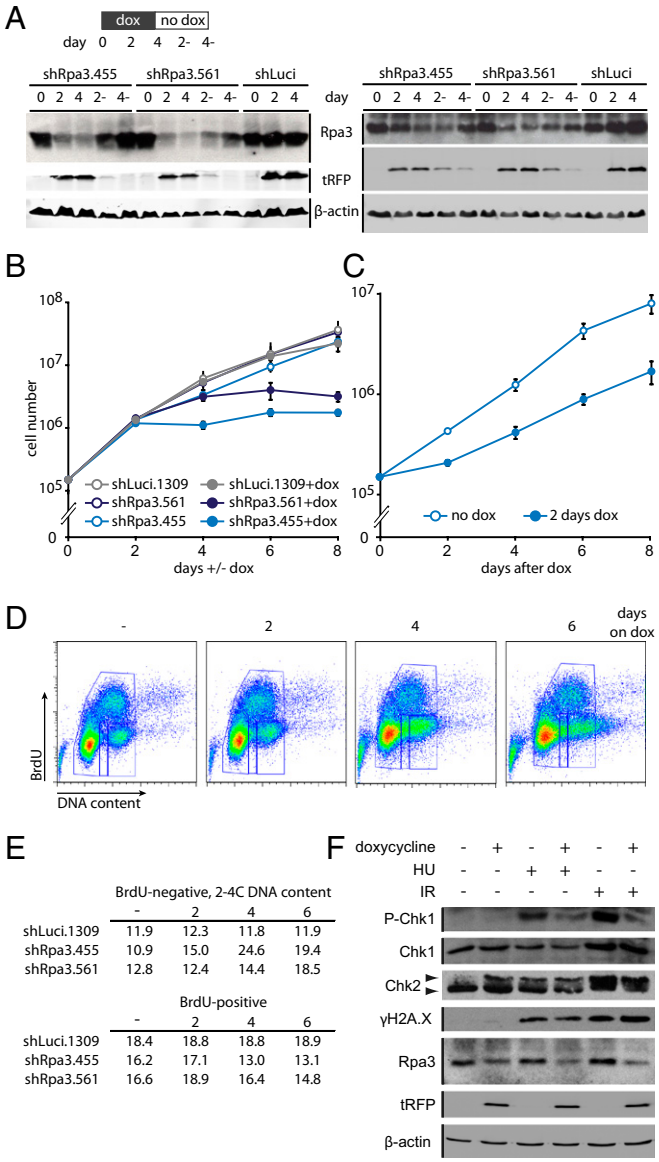

Fig. 2. Dox-inducible shRpa3 results in rapid, reversible Rpa3 knockdown and a defect in cell proliferation and Chk1 signaling. (*A*) Immunoblot of Rosa-rtTA;TtR-shRpa3 or Rosa-rtTA;TtR-shLuci cells. (*Left*) ES cells. (*Right*) MEFs. A time course over 4 d of dox treatment and 4 d of subsequent dox withdrawal is shown. (*B*) Growth curve of Rosa-rtTA;TtR-shRpa3 or Rosa-rtTA;TtR-shLuci transgenic MEFs, grown with or without dox. (*C*) Growth curve of Rosa26-rtTA;TtR-shRpa3.455 MEFs passaged with or without dox for 2 d before day 0. After day 0, all cells were cultured without dox. (*D*) Representative cell cycle analysis of Rosa-rtTA;TtR-shRpa3.455 MEFs grown in media containing dox for 0, 2, 4, or 6 d. (*E*) Quantification of cell cycle analysis in Rosa-rtTA;TtRM MEFs. (*F*) Immunoblot in Rosa-rtTA;TtR-shRpa3.455 MEFs treated with or without dox for 4 d. After 4 d dox treatment, cells were treated with hydroxyurea (HU) or ionizing radiation (IR).

cells treated with dox for 4 d before HU or IR, Chk1 phosphorylation was abrogated, whereas Chk2 and H2A.X phosphorylation were unaffected. These data demonstrate that Rpa3 knockdown can impede Chk1 signaling, consistent with previous work showing that the Rpa complex is required for recruitment and activation of ATR kinase at sites of DNA damage (27, 28). Thus, inducible knockdown of Rpa in vitro recapitulates known loss of function phenotypes, demonstrating that our system is suitable for further characterization of this and other essential genes.

Adult CMV-rtTA;Rosa-rtTA;shRpa3 and Rosa-rtTA$^{+/+}$;shRpa3 Mice Exhibit Rapid Weight Loss Upon Dox Treatment. A key advantage of inducible shRNA transgenics targeting essential genes is to bypass embryonic lethality and examine the impact of inducible gene knockdown at later stages of development or in the adult. Consistent with the ongoing need for cell proliferation during embryogenesis, bitransgenic Rosa-rtTA;TtR-shRpa3 animals died shortly after birth when treated with dox in utero. Surprisingly, if Rosa-rtTA;TtR-shRpa3 mice were treated with dox at adulthood (6 wk of age), no overt phenotype was observed. Notably, fluorescent reporter expression was much lower in adults than in embryos and substantially more tissue-restricted, suggesting that this discrepancy might arise from insufficient shRNA expression rather than a reduced requirement for Rpa3 in the adult. When shRpa3 mice were crossed to the CMV-rtTA strain (24) and treated with dox at 6 wk of age, fluorescence was observed in more widespread tissues but still no obvious phenotype resulted. However, when mice were triple transgenic CMV-rtTA;Rosa-rtTA;shRpa3 or Rosa-rtTA;Rosa-rtTA;shRpa3 (Rosa-rtTA$^{+/+}$;shRpa3), shRNA induction by dox treatment led to cell cycle arrest and caused rapid weight loss, even in the case of weak shRpa3.429 (Fig. 3).

Although shRpa3-induced weight loss led to death in most cases, some mice regained weight and survived while continuously treated with dox (Fig. S3 *A* and *B*). Only mice with strong Rpa3 shRNAs that were homozygous for Rosa-rtTA (Rosa-rtTA$^{+/+}$;TtR-shRpa3) never survived dox treatment at 6 wk of age (Fig. S3*A*). We hypothesized that less penetrant phenotypes could be due to weak or mosaic shRNA expression, which would lead to the outgrowth of cells that did not efficiently induce the shRNA (see also ref. 29). Consistent with this notion, Rosa-rtTA$^{+/+}$ mice show higher expression of tRFP than Rosa-rtTA$^{+/-}$ in many tissues, as well as expression in a greater number of cells per tissue than Rosa-rtTA$^{+/-}$ (Fig. S4*A*). Furthermore, multiple tissues of Rosa-rtTA;TtR-shRpa3 and CMV-rtTA;Rosa-rtTA;TtR-shRpa3 mice that survived long-term dox treatment were less tRFP-positive than those in treated shLuci counterparts (Fig. S4 *B* and *C*), suggesting that selection occurs against shRpa3 expression but not against neutral shLuci. Therefore, the expression pattern of the tet-transactivator, and in turn, the TRE-driven shRNA, influences the extent of phenotype in this system.

shRpa3 Induces Severe Intestinal Villus Atrophy and a Transient Hematopoietic Defect in Rosa26-rtTA$^{+/+}$;TtR-shRpa3 Mice. To examine the effect of Rpa3 knockdown on adult mice, we further characterized the most robust phenotype in detail. Rosa-rtTA$^{+/+}$;TtR-shRpa3 mice consistently lost weight after 3–5 d of dox food and became moribund around day 8 (Fig. 4*A*). Control Rosa-rtTA$^{+/+}$;TtR-shLuci mice continued to gain weight at a rate typical of 6-wk-old animals. Dramatic total weight loss was accompanied by moderate decrease in size and weight of individual organs such as the liver, kidneys, and spleen (Fig. S5*A*).

To determine which systems were most likely affected by shRNA expression in Rosa-rtTA$^{+/+}$;TtR mice, we assessed tRFP fluorescence throughout the body. Based on tRFP levels, Rosa-rtTA$^{+/+}$ drove TRE expression in many tissues including skin, bone marrow, spleen and pancreas, but levels were highest in the intestine. Accordingly, histology revealed the rapid degeneration of the intestinal epithelium in Rosa-rtTA$^{+/+}$;TtR-shRpa3 mice over the time course of dox treatment (Fig. 4*C*). Immunohistochemistry for tRFP shows strong expression of the tRFP-shRNA cassette by day 3 on dox (Fig. 4*C*). Rpa3 knockdown in the intestine is observed by 5 d on dox, as was a reduction in proliferating cells and BrdU incorporation (Fig. 4 *B–D* and Fig. S6 *A* and *B*). By day 7, intestinal architecture is severely disrupted, and Ki67-positive cells are reduced by fourfold (Fig. 4 *C* and *D*). Rpa3 shRNA did not cause a significant increase in apoptotic cells in the intestine (Fig. S6*C*). Importantly, this effect was not due to overexpression of an exogenous miR, as the expression of a luciferase shRNA had no effect on intestinal proliferation or architecture (Fig. 4 *C* and *D* and Fig. S6 *A* and *B*). Two independent Rpa3 shRNAs show the same effect, ruling out off-

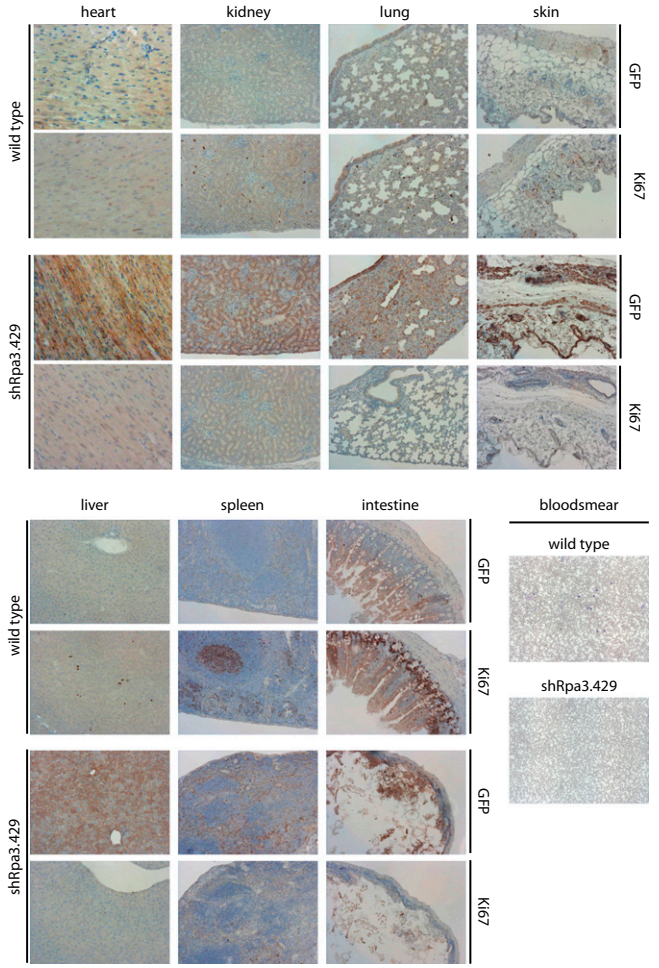

Fig. 3. shRpa3.429 induction causes cell cycle arrest in many tissues in CMV-rtTA;Rosa-rtTA;TG-shRpa3.429 mice. GFP and Ki67 immunohistochemistry in CMV-rtTA;Rosa-rtTA;TG-shRpa3.429 mice treated with dox for 14 d. Wild-type control mouse is also shown.

target effects of a single shRNA (Fig. 4 *C* and *D* and Figs. S5*A* and S6 *A* and *B*).

In the bone marrow of Rosa-rtTA$^{+/+}$;TtR-shRpa3 mice, erythroid precursors are severely depleted after 3 d on dox food compared with shLuci controls (Fig. 4*E*). This effect is transient and does not lead to a significant anemia in the periphery. Also, no significant change in overall BrdU incorporation was observed in the bone marrow. We hypothesized that the transience of this phenotype might be due to compensation by cells that fail to express the shRNA cassette. In the bone marrow of control shLuci mice, 35–67% cells were tRFP-positive. Consistent with a rapid selection against shRpa3 expression, tRFP-positive cells were relatively depleted in the bone marrow of shRpa3 mice treated with dox (8–26%, Fig. 4*F*). Thus, the fluorescent reporter can be used as a read-out of cell-autonomous effects of knockdown in tissues where expression of the tRFP-shRNA transcript is mosaic.

Weight Loss and Villus Atrophy in Rosa-rtTA$^{+/+}$;TtR-shRpa3 Mice Are Reversible. Because shRpa3-induced cell cycle arrest was reversible in vitro, we aimed to determine whether the effects of shRpa3 expression were reversible in vivo, and if dox withdrawal could rescue weight loss and tissue defects in this model. Therefore, 6-wk-old Rosa-rtTA$^{+/+}$;TtR-shRpa3 mice were treated with a 3-d pulse of dox food and then returned to a dox-free diet. These mice exhibited a delay in weight gain relative to shLuci controls and mild weight loss but eventually regained weight at a rate

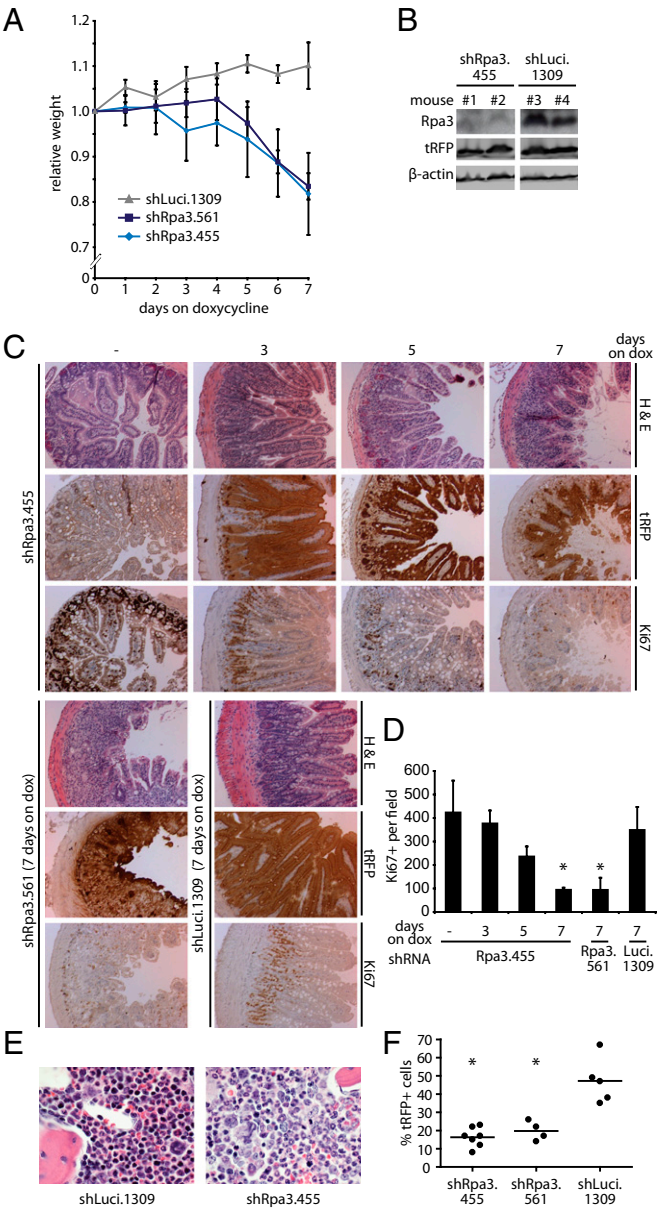

Fig. 4. shRpa3 induction in Rosa-rtTA$^{+/+}$;TtR-shRpa3 mice causes weight loss, cell cycle arrest, and atrophy of the intestinal epithelium. (*A*) Weight loss/gain in Rosa26-rtTA$^{+/+}$;TtRM mice treated with dox food at 6 wk of age. (*B*) Immunoblot of intestinal epithelial cells from Rosa26-rtTA$^{+/+}$;TtRM mice treated with dox for 5 d. Lysates from two different mice for each shRNA are shown. (*C*) Histology and immunohistochemistry on intestines of 6-wk-old Rosa26-rtTA$^{+/+}$;TtRM mice treated with dox for 0, 3, 5, or 7 d. (*D*) Quantification of intestinal Ki67 staining. Each time point shown represents the mean of three mice. Error bars are SD. *$P < 0.05$, compared with untreated shRpa3.455 mice. (*E*) Histology of bone marrow from Rosa26-rtTA$^{+/+}$;TtRM mice treated with dox for 3 d. shRpa3 marrow shows a marked decrease in dark-staining erythroid precursors compared with shLuci. (*F*) Quantification of tRFP-positive cells in bone marrow of Rosa-rtTA$^{+/+}$;TtRM mice treated with dox. (Values from 3-, 5-, or 7-d dox are combined.) *$P < 0.0005$.

similar to controls (Fig. 5*A*). In CMV-rtTA;Rosa-rtTA;TG-shRpa3.429 mice, which could be left on dox longer (10 d), a more marked weight loss and subsequent regain was observed upon dox withdrawal (Fig. S7).

Again, we extended our characterization of this recovery in the most penetrant Rosa-rtTA$^{+/+}$;TtR-shRpa3 model. Here, 5 d after beginning dox treatment (2 d after dox withdrawal), the intestinal epithelium showed moderate atrophy and loss of proliferating

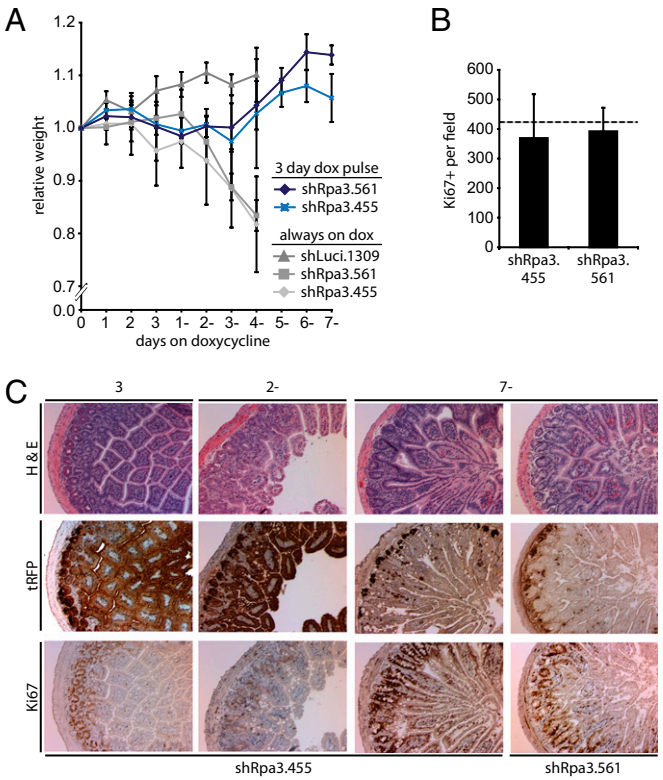

Fig. 5. shRpa3-induced weight loss and villus atrophy are reversible. (*A*) Relative weight in Rosa26-rtTA$^{+/+}$;TtRM mice treated with a 3-d pulse of dox food at 6 wk of age. (*B*) Quantification of Ki67-positive cells in intestines of mice treated for 3 d with dox, then allowed to recover for 7 d. Mean is shown ($n = 3$ mice); error bars are SD. Dotted line represents the mean Ki67^{+} per field in untreated shRpa3.455 mice. (*C*) Histology and immunohistochemistry on a 7-d time course of recovery following a 3-d pulse of dox treatment.

cells similar to that in mice treated with dox continually for 5 d (Figs. 4*C* and 5*C*). By 7 d after dox withdrawal, tRFP expression was diminished (Fig. 5*C*), demonstrating extinguished TRE-tight expression. At this time point, mice had recovered a normal number of proliferating cells in the intestine and normal tissue architecture, and liver, kidney, and spleen weights were comparable to controls (Fig. 5 *B* and *C* and Fig. S5*B*). Thus, the effects of Rpa3 knockdown were fully reversible upon shRpa3 withdrawal. Hence, our system shows that transient inactivation of the replication gene Rpa3 causes a reversible inhibition of DNA synthesis but is not invariably lethal, thus providing a system to study this essential process at different developmental stages and, through the use of tissue specific tranactivators, in particular cell types. More broadly, our study provides a platform and blueprint to suppress and reactivate any essential gene in vivo.

Discussion

Here, we establish that an inducible RNAi transgenic system is useful to study genes that are essential in adult tissues. By targeting cell proliferation, we showed that this system is sufficiently robust to examine deleterious phenotypes induced by knockdown. Importantly, we used a fluorescent protein encoded on the same transcript as the shRNA to tightly report the level of shRNA induction at single cell resolution. This feature highlights which tissues are most likely to exhibit a phenotype caused by knockdown and aids in the interpretation of negative results by providing a simple test of whether the shRNA was expressed. In future studies, the reporter could even be used to study cell-autonomous effects of knockdown by examining only the fluorescent cells in tissues where shRNA expression is variegated.

Still, many applications of inducible shRNA transgenics require knockdown throughout the tissue of interest. Here, we observed that CMV-rtTA;Rosa-rtTA;shRpa3 mice sometimes regained weight and survived following an initial weight loss, suggesting that a small number of cells that fail to induce or actively silence rtTA or TRE expression can compensate for arrested cells in which shRNA expression is maintained. Accordingly, analysis of the intestines of surviving mice for the shRNA-linked fluorescence reporter indicated that they consisted largely of nonfluorescent cells. Hence, moving forward, more transactivator strains that drive high levels of truly ubiquitous expression from the TRE must be developed. Our group has already generated a superior strain to Rosa-rtTA for driving shRNA expression in widespread adult tissues (17); one allele of this transgene, which drives expression of an optimized rtTA (rtTA3) from the CMV early enhancer/chicken β actin (CAG) promoter is sufficient to induce weight loss and death in combination with either a strong or weak shRpa3.

Rpa3 knockdown in CMV-rtTA;Rosa-rtTA;shRpa3 mice disrupted the intestine more than any other tissue; this is likely due to both (*i*) strong and penetrant expression of the shRNA cassette and (*ii*) the high rate of cell turnover in this tissue. Because shRNA led to lethality in only 8 d in this model, other tissues might also be dramatically affected by shRNA expression over a longer time scale. The construction of our system allows shRNA transgenic mice to be crossed to tissue-specific transactivators to examine the effect of inducible knockdown in restricted compartments. Again, although numerous tissue-specific transactivator strains exist, many drive mosaic TRE expression within the tissue of interest, so a fluorescent reporter is also indispensable in these backgrounds. As improved ubiquitous and tissue-specific transactivators are developed, dox delivery and TRE accessibility may also be limiting to shRNA expression in some tissues.

The strong antiproliferative effect of shRPA3 was evident in a library of shRNAs targeting DNA replication and cell cycle regulated genes in the cancer cell line HCT116. This may be because RPA is required for DNA replication, DNA repair, and cell cycle checkpoint processes (21). Consistent with this finding, ribonucleotide reductase (RRM1) is also involved in all three processes and was also identified in the screen. Thus, directly targeting the many roles of RPA is a powerful genetic means to cause reversible cell cycle arrest that does not lead to apoptosis. In transgenics, this provides an interesting tool to study normal tissue maintenance at any stage of development and, with a transient pulse of knockdown, the process of tissue regeneration. For these applications, shRpa3 mice are an interesting complement to existing cell lineage ablation technologies, such as diphtheria toxin or toxin receptor expression (30–32). Targeting other essential genes will require careful assessment of shRNA potency because shRNAs against subunits of the Origin Recognition Complex required > 90% knockdown of protein levels to prevent proliferation of HCT116 cells.

More broadly, transient inactivation of essential genes in the whole organism is an exciting prospect for mouse genetics. On a practical level, our platform can be modified through simple cloning to target any gene, leading to transgenic mice within ~4 mo, up to three times faster than standard gene targeting approaches. More importantly, the ability to toggle gene expression at any developmental stage and examine the outcome later in development is a major advance over conditional gene deletion, which is not reversible. A systemic pulse of gene knockdown is also the closest genetic approximation to a single treatment with a targeted small molecule-based therapy that incompletely inhibits gene function. Thus, this system will be invaluable for testing the efficacy and side effects of inhibiting novel therapeutic targets. In general, this level of genetic malleability brings mouse genetics forward to meet that of other model organisms, which have long used temperature-sensitive mutations to this end. Adding a new layer of versatility, the sequence-specific nature of RNAi allows the rational targeting of any gene of interest inducibly and reversibly.

Materials and Methods

RNAi Screening. shRNAs from Open Biosystems were subcloned into a puromycin-selectable retroviral expression vector (for cloning details, please see *SI Text*). HCT116 cells were transduced with viral supernatant produced by amphotropic phoenix packaging cells and replated into selection media (DMEM supplemented with 10% FBS containing 1.5 μg/mL puromycin). After 24 h, cells were replated in media containing puromycin and were counted after another 96 h. To confirm shRpa3 effects, HCT116 cells transduced with pLM-puro-shRpa3 or shLuci.203 were plated at 100,000 cells per well in a six-well plate in media containing 1.5 μg/mL puromycin, and one well of cells was resuspended and counted each day after plating.

Transgenic Alleles and in Vivo Dox Treatment. Mouse shRpa3.455 was obtained from Open Biosystems in pSM2. shRpa.429 was designed using the BIOPRED*si* prediction algorithm (33). shRpa3.561 was identified through a tiling assay to identify potent shRNAs (26). shLuci.1309 was provided by Gregory Hannon (Cold Spring Harbor Laboratory). All shRNAs were subcloned into the targeting vectors by digestion with XhoI and EcoRI, and sequences are listed in Table S1. All transgenic strains used are listed in Table S2. Mice were fed food containing dox (625 mg/kg; Harlan Laboratories). Embryos were treated in utero by feeding pregnant females dox food at embryonic day 15–17.

Cell Culture. KH2 ES cells were cultured and electroporated according to protocols modified from (22); also see *SI Text*. For Western blot samples, targeted ES cells were maintained in 50 μg/mL hygromycin and 2.5 μg/mL puromycin. MEFs were harvested and as described (34), and cultured in low-oxygen conditions (1.5% O_2) in DMEM with 10% FBS, 50 μg/mL hygromycin and 2.5 μg/mL puromycin. Growth curves were performed by serially plating 150,000 cells in one well of a six-well plate. All dox-containing media were prepared at 1 μg/mL dox (Sigma-Aldrich).

Annexin V Staining and Cell Cycle Analysis. APC-conjugated Annexin V (BD Biosciences) was used according to the manufacturer's specifications. For cell cycle analysis, MEFs were pulsed with BrdU at 10 μM for 4 h and subsequently stained with APC-conjugated BrdU antibody (BD Biosciences) and DAPI. Flow cytometry was performed on a LSRII cell analyzer (Becton Dickinson) and processed with FlowJo analysis software (TreeStar).

Immunoblots. Antibodies used were Rpa3 (M-18, Santa Cruz Biotechnology), tRFP (Evrogen), β-actin (AC-15; Sigma-Aldrich), Chk1 (DCS-310; Santa Cruz Biotechnology), phospho-Chk1 (133D3; Cell Signaling Technology), Chk2 (611570; BD Biosciences), and gamma-H2A.X (#2577; Cell Signaling Technology). Also see *SI Text*.

Immunostaining. Antigen retrieval was performed in Trilogy buffer (Cell Marque) according to manufacturer's protocol. Immunohistochemistry was performed using the Epitomics ACE detection kit. Primary antibodies used were: Ki67 (rabbit anti-mouse; Dianova), tRFP (Evrogen), and cleaved caspase 3 (#9661; Cell Signaling).

ACKNOWLEDGMENTS. We gratefully acknowledge Christof Fellmann for providing RNAi reagents and technical recommendations. We thank Uli Bialucha, Maarten Hoek, June-Hee Park, Khalid Siddiqui, and Hiroyuki Takai for providing protocols and helpful discussions. We are grateful to the Research Animal Diagnostic Laboratory for tissue processing and histology and to Scott Kogan and Carlos Cordon Cardo for pathology. This work was supported by generous gifts from the Don Monti Memorial Research Foundation and National Institutes of Health Program Project Grant 5P01 CA 013106. K.M. was the Robert and Teresa Lindsay Fellow of Watson School of Biological Sciences. A.M. is supported by a grant from the Alan and Lola Goldring Foundation. J.Z. was the Andrew Seligson Memorial Fellow at Cold Spring Harbor Laboratory, and L.E.D. is supported by an Overseas Biomedical Research Fellowship of the National Health and Medical Research Council of Australia. S.W.L. is a Howard Hughes Medical Institute investigator.

1. Sage J, Miller AL, Pérez-Mancera PA, Wysocki JM, Jacks T (2003) Acute mutation of retinoblastoma gene function is sufficient for cell cycle re-entry. *Nature* 424:223–228.
2. Schmidt-Supprian M, Rajewsky K (2007) Vagaries of conditional gene targeting. *Nat Immunol* 8:665–668.
3. Loonstra A, et al. (2001) Growth inhibition and DNA damage induced by Cre recombinase in mammalian cells. *Proc Natl Acad Sci USA* 98:9209–9214.
4. Forni PE, et al. (2006) High levels of Cre expression in neuronal progenitors cause defects in brain development leading to microencephaly and hydrocephaly. *J Neurosci* 26:9593–9602.
5. Silver DP, Livingston DM (2001) Self-excising retroviral vectors encoding the Cre recombinase overcome Cre-mediated cellular toxicity. *Mol Cell* 8:233–243.
6. Dickins RA, et al. (2007) Tissue-specific and reversible RNA interference in transgenic mice. *Nat Genet* 39:914–921.
7. Nyabi O, et al. (2009) Efficient mouse transgenesis using Gateway-compatible ROSA26 locus targeting vectors and F1 hybrid ES cells. *Nucleic Acids Res* 37:e55.
8. Christoph T, et al. (2008) Investigation of TRPV1 loss-of-function phenotypes in transgenic shRNA expressing and knockout mice. *Mol Cell Neurosci* 37:579–589.
9. Seibler J, et al. (2007) Reversible gene knockdown in mice using a tight, inducible shRNA expression system. *Nucleic Acids Res* 35:e54.
10. Yang W, Paschen W (2008) Conditional gene silencing in mammalian cells mediated by a stress-inducible promoter. *Biochem Biophys Res Commun* 365:521–527.
11. Carmell MA, Zhang L, Conklin DS, Hannon GJ, Rosenquist TA (2003) Germline transmission of RNAi in mice. *Nat Struct Biol* 10:91–92.
12. Lu W, Yamamoto V, Ortega B, Baltimore D (2004) Mammalian Ryk is a Wnt coreceptor required for stimulation of neurite outgrowth. *Cell* 119:97–108.
13. Rubinson DA, et al. (2003) A lentivirus-based system to functionally silence genes in primary mammalian cells, stem cells and transgenic mice by RNA interference. *Nat Genet* 33:401–406.
14. Seibler J, et al. (2005) Single copy shRNA configuration for ubiquitous gene knockdown in mice. *Nucleic Acids Res* 33:e67.
15. Dickins RA, et al. (2005) Probing tumor phenotypes using stable and regulated synthetic microRNA precursors. *Nat Genet* 37:1289–1295.
16. Stegmeier F, Hu G, Rickles RJ, Hannon GJ, Elledge SJ (2005) A lentiviral microRNA-based system for single-copy polymerase II-regulated RNA interference in mammalian cells. *Proc Natl Acad Sci USA* 102:13212–13217.
17. Premsrirut PK, (2011) et al. A rapid and scalable system for studying gene function in mice using conditional RNA interference. *Cell* 145:145–158.
18. Lapik YR, Fernandes CJ, Lau LF, Pestov DG (2004) Physical and functional interaction between Pes1 and Bop1 in mammalian ribosome biogenesis. *Mol Cell* 15:17–29.
19. Kinoshita Y, et al. (2001) Pescadillo, a novel cell cycle regulatory protein abnormally expressed in malignant cells. *J Biol Chem* 276:6656–6665.
20. Zou Y, Liu Y, Wu X, Shell SM (2006) Functions of human replication protein A (RPA): from DNA replication to DNA damage and stress responses. *J Cell Physiol* 208: 267–273.
21. Wold MS (1997) Replication protein A: a heterotrimeric, single-stranded DNA-binding protein required for eukaryotic DNA metabolism. *Annu Rev Biochem* 66:61–92.
22. Beard C, Hochedlinger K, Plath K, Wutz A, Jaenisch R (2006) Efficient method to generate single-copy transgenic mice by site-specific integration in embryonic stem cells. *Genesis* 44:23–28.
23. Hochedlinger K, Yamada Y, Beard C, Jaenisch R (2005) Ectopic expression of Oct-4 blocks progenitor-cell differentiation and causes dysplasia in epithelial tissues. *Cell* 121:465–477.
24. Gossen M, et al. (1995) Transcriptional activation by tetracyclines in mammalian cells. *Science* 268:1766–1769.
25. Agha-Mohammadi S, et al. (2004) Second-generation tetracycline-regulatable promoter: repositioned tet operator elements optimize transactivator synergy while shorter minimal promoter offers tight basal leakiness. *J Gene Med* 6:817–828.
26. Fellmann C, et al. (2011) Functional identification of optimized RNAi triggers using a massively parallel Sensor assay. *Mol Cell* 41:733–746.
27. Choi JH, et al. (2010) Reconstitution of RPA-covered single-stranded DNA-activated ATR-Chk1 signaling. *Proc Natl Acad Sci USA* 107:13660–13665.
28. Zou L, Elledge SJ (2003) Sensing DNA damage through ATRIP recognition of RPA-ssDNA complexes. *Science* 300:1542–1548.
29. Zuber J, et al. (2011) Toolkit for evaluating genes required for proliferation and survival using tetracycline-regulated RNAi. *Nat Biotechnol* 29:79–83.
30. Breitman ML, et al. (1987) Genetic ablation: targeted expression of a toxin gene causes microphthalmia in transgenic mice. *Science* 238:1563–1565.
31. Palmiter RD, et al. (1987) Cell lineage ablation in transgenic mice by cell-specific expression of a toxin gene. *Cell* 50:435–443.
32. Saito M, et al. (2001) Diphtheria toxin receptor-mediated conditional and targeted cell ablation in transgenic mice. *Nat Biotechnol* 19:746–750.
33. Huesken D, et al. (2005) Design of a genome-wide siRNA library using an artificial neural network. *Nat Biotechnol* 23:995–1001.
34. McCurrach ME, Lowe SW (2001) Methods for studying pro- and antiapoptotic genes in nonimmortal cells. *Methods Cell Biol* 66:197–227.